PALEONTOLOGY

Biomechanical simulations reveal a trade-off between adaptation to glacial climate and dietary niche versatility in European cave bears

Alejandro Pérez-Ramos[1]*, Z. Jack Tseng[2], Aurora Grandal-D'Anglade[3], Gernot Rabeder[4], Francisco J. Pastor[5], Borja Figueirido[1]*

The cave bear is one of the best known extinct large mammals that inhabited Europe during the "Ice Age," becoming extinct ≈24,000 years ago along with other members of the Pleistocene megafauna. Long-standing hypotheses speculate that many cave bears died during their long hibernation periods, which were necessary to overcome the severe and prolonged winters of the Last Glacial. Here, we investigate how long hibernation periods in cave bears would have directly affected their feeding biomechanics using CT-based biomechanical simulations of skulls of cave and extant bears. Our results demonstrate that although large paranasal sinuses were necessary for, and consistent with, long hibernation periods, trade-offs in sinus-associated cranial biomechanical traits restricted cave bears to feed exclusively on low energetic vegetal resources during the predormancy period. This biomechanical trade-off constitutes a new key factor to mechanistically explain the demise of this dominant Pleistocene megafaunal species as a direct consequence of climate cooling.

INTRODUCTION

The cave bear (*Ursus spelaeus* s.l.) is an extinct species of the Pleistocene megafauna that inhabited Europe during the Last Glacial Period (LGP), and it is one of the best known extinct species that lived alongside prehistoric humans. A long-standing hypothesis suggests that cave bears were more dependent on caves than their closest relative, the living brown bear (*Ursus arctos*) [e.g., (*1*)]. A recent analysis of mitochondrial DNA revealed that cave bears had extreme fidelity to their birth sites, and they formed stable maternal social groups for the purpose of hibernation, returning to the same cave every winter (*2*). Furthermore, cave bears had longer hibernation periods than other living bears to overcome the long and cold winters of the LGP [e.g., (*3*)]. Their high dependency on cave shelters explains why Late Pleistocene caves of Europe have yielded a huge number of fossil remains of bears that likely died during hibernation, the accumulation of these fossils occurring over periods of hundreds or even thousands of years (*1*, *4*). Although mortality for the older individuals is usually attributed to either accidents, illness, or a lack of sufficient fat storage to endure winter hibernation [e.g., (*5*)], it has also been proposed that humans competed for cave sites with cave bears. Archeological records show cut marks in cave bear remains from several sites attributed to human processing of bear bones [e.g., (*6*)]. On the basis of this evidence, competition for resources and direct hunting by *Homo* in Europe are among the prevailing hypotheses to explain a human-driven cave bear decline [e.g., (*7*)].

Climate cooling explains the demise of the cave bear during the coldest phase of the LGP (*8*). Biogeochemical studies of bone collagen suggest that cave bears were adapted to feed exclusively on vegetal resources from 100,000 to 20,000 years ago (*9*). However, there is no evidence of a dietary shift toward omnivory when vegetation productivity lowered as a consequence of climate cooling during the beginning of the Last Glacial Maximum (*10*). This lack of dietary flexibility may have been a critical factor in the decline of the last populations of cave bears (*9*), intensified by human competition for cave space (*11*), to cause the extinction of the species at the beginning of the Last Glacial Maximum (~24,000 years ago).

Here, we investigate whether cave bears were biomechanically restricted to feed exclusively on vegetal resources using three-dimensional (3D) computer simulations of different feeding scenarios. As the sinuses (Fig. 1) play a key role in the control of hibernation (*12*–*15*), we specifically address the impact of large sinuses in cave bear feeding biomechanics by comparing skull models with sinuses and with artificially removed sinuses.

RESULTS

FEA with sinuses

Here, we calculated the values of strain energy (SE; a measure of skull stiffness or structural stability) and of mechanical efficiency (ME) using finite element analysis (FEA) in all species of living bears and cave bears (*U. spelaeus* s.l.) (Fig. 1 and table S1). The results of both SE and ME computed for all biting scenarios at a gape angle of 12° (Fig. 2) are shown in fig. S1 and tables S2 and S3.

The difference between the values in ME obtained for the canine and second molar (mΔME), as well as the differences between the maximum and minimum values of adjusted SE across all teeth simulations (mΔSEa), is shown in table S6. This informs us on the functional differentiation of the dentition—i.e., higher maximum differences indicate a higher degree of functional differentiation across the tooth row and therefore more restrictive diets. In contrast, lower maximum differences indicate a lower degree of functional differentiation across the tooth row and therefore more flexible diets (*16*). A bivariate plot of mΔSEa against mΔME is shown in Fig. 3A. Whereas *Ailuropoda melanoleuca* has the greatest mΔME (0.27 ± 0.02), indicating a large

[1]Departamento de Ecología y Geología, Facultad de Ciencias, Universidad de Málaga, 29071 Málaga, Spain. [2]Department of Pathology and Anatomical Sciences, Jacobs School of Medicine and Biomedical Sciences, University at Buffalo, Buffalo, NY 14203, USA. [3]Instituto Universitario de Xeoloxia, Universidade da Coruña, Coruña, Spain. [4]University of Vienna, Institute of Palaeontology and Naturkundliche Station Lunz am See, Vienna, Austria. [5]Departamento de Anatomía y Radiología, Universidad de Valladolid, Valladolid 47005, Spain.
*Corresponding author. Email: pera@uma.es (A.P.-R.); borja.figueirido@uma.es (B.F.)

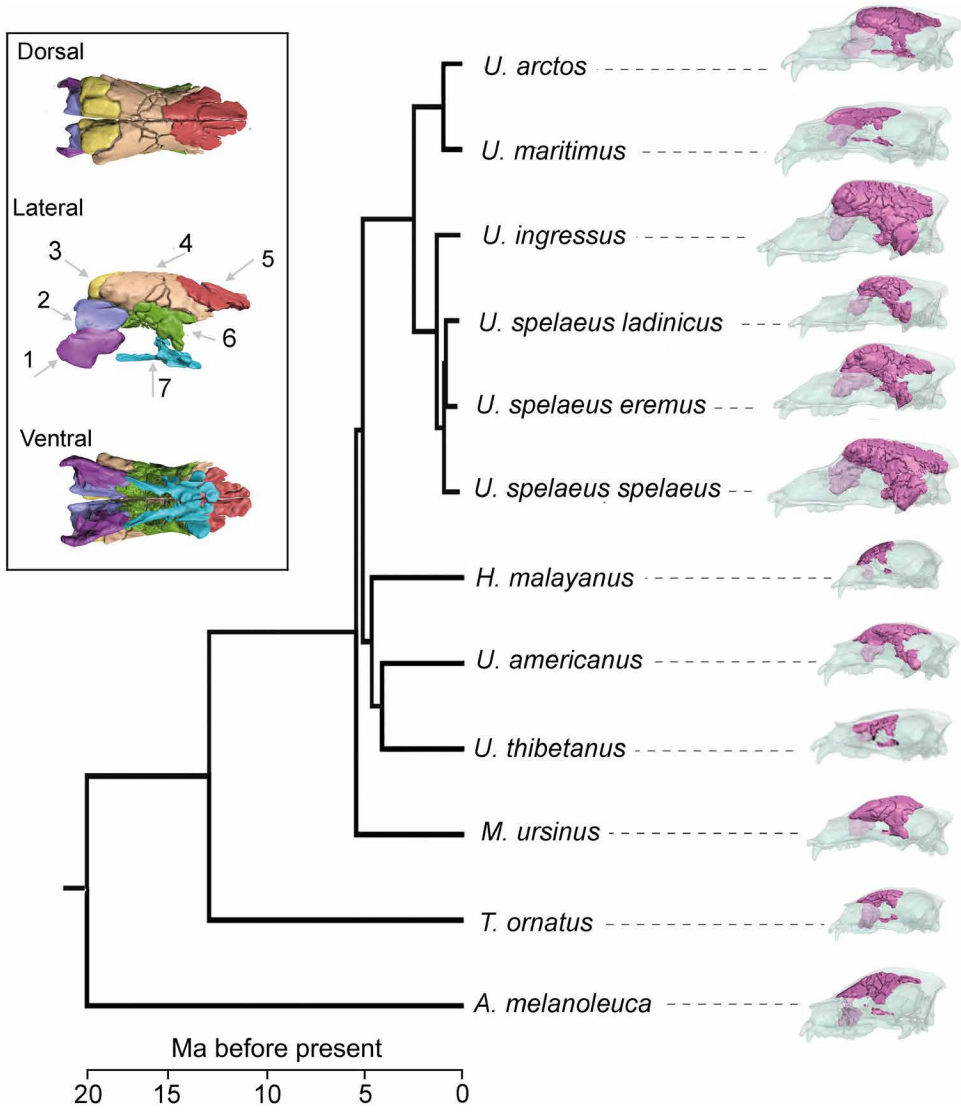

Fig. 1. Paranasal sinus anatomy and assembled phylogeny for all living bear species and cave bears. The phylogeny (i.e., tree topology, branch lengths, and divergence times) is taken from (*24*). The 3D model of the paranasal sinus (within the box) belongs to *U. arctos*. 1, maxillary sinus; 2, nasomaxillary sinus; 3, rostro-frontal sinus; 4, mediolateral frontal sinus; 5, caudo-sagittal frontal sinus; 6, ethmoid-lateral sinus; 7, palatine-sphenoid sinus. Sinus anatomy is based on (*40*). Ma, million years.

functional differentiation among teeth, the values for the rest of the species range between 0.13 ± 0.02 (for *U. arctos*) and 0.19 ± 0.02 (for *Helarctos malayanus*). The values of mΔSEa among living bears range from values of 0.14 ± 0.03 (for *Ursus americanus*) and from values of 0.40 ± 0.02 for *A. melanoleuca* (Fig. 3A), indicating higher differences in resisting stresses with different teeth. Cave bears have a range in mΔME from 0.14 ± 0.01 (for *U. spelaeus spelaeus*) to 0.18 ± 0.01 (for *U. spelaeus ladinicus*). The values of mΔSEa in cave bears are among the highest of all bears, ranging from 0.46 ± 0.01 (for *U. spelaeus ladinicus*) to 0.31 ± 0.01 for *U. spelaeus eremus*, and only comparable to the living *A. melanoleuca* and *Melursus ursinus* (Fig. 3A). This indicates that cave bears have similar values of mechanical advantage to extant bears, but in general, they have higher differences in resisting stresses with different teeth.

The von Mises stress distribution across the skulls in all of the living species indicates that the stress is distributed along the frontal region of the skull, from the anterior part of the rostrum to the anterior part of the neurocranium, as well as at the temporo-mandibular joint (TMJ). The species with the highest stresses in all feeding scenarios are *M. ursinus* and *U. americanus*. In contrast, the species with the lowest stresses across all scenarios are *A. melanoleuca* and *Ursus thibetanus*, followed by *Tremarctos ornatus* and *H. malayanus* (Fig. 4A). The pattern of stress distribution in cave bears is similar to the living species—i.e., affecting the frontal region and the TMJ—but in these taxa, the stress is not distributed continuously from rostrum to neurocranium (Fig. 4B). The species with the highest stresses in all scenarios is *U. spelaeus eremus*, and the species with the lowest stresses is *U. spelaeus spelaeus*. Moreover, the stresses are substantially higher at the TMJ in all cave bears than in living bears, with the exception of *H. malayanus* and *U. americanus*. Among cave bears, the taxa with the highest stresses at the TMJ are *U. spelaeus ladinicus* and *Ursus ingressus*, and the species with the lowest stresses is *U. spelaeus eremus*. Moreover, it is noteworthy that all cave bears exhibit less stress on all molar biting scenarios than with the canine and fourth premolar

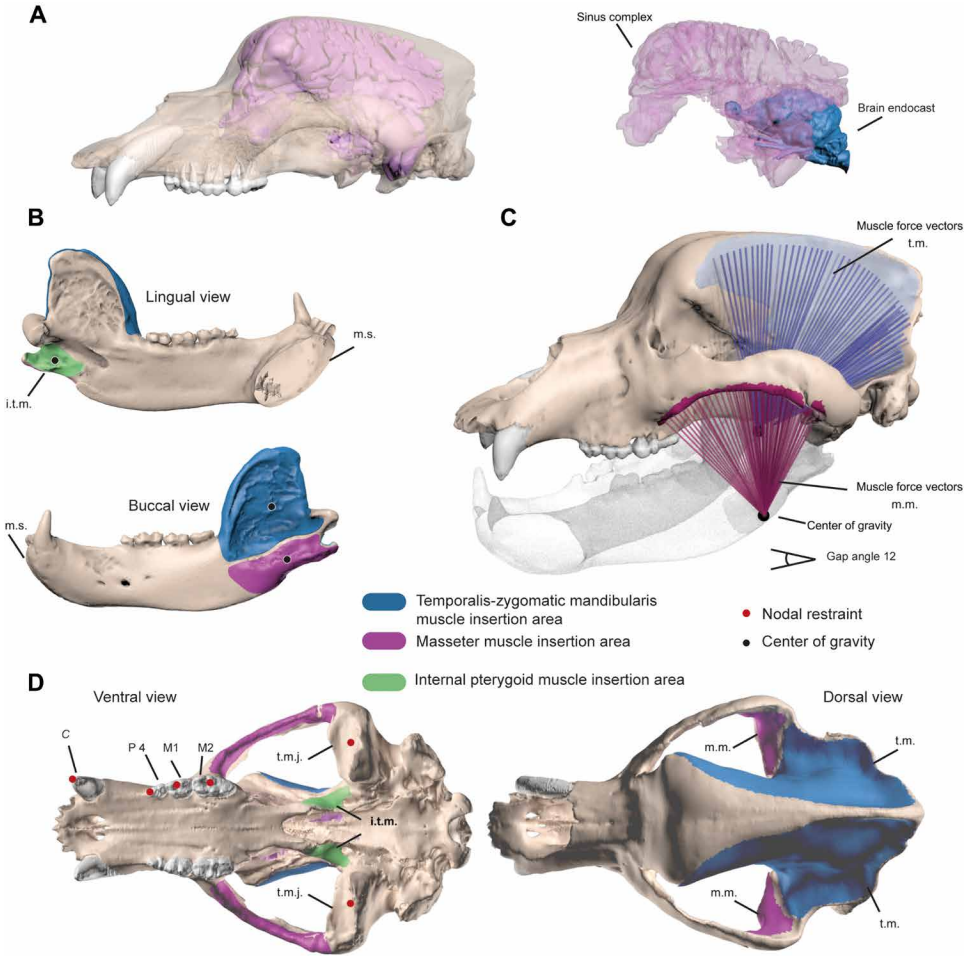

Fig. 2. Biomechanical settings for FEAs using the 3D model of *U. ingressus* as an example. (**A**) Model of *U. ingressus* skull showing the disposition of the sinuses in the frontal dome (left) and its topographical relationship with the brain. (**B**) Centers of gravity (black circles) of mandible muscle insertion areas. Centers of gravity are represented by black circles. (**C**) Simulation of loading muscle forces used in biomechanical simulations and obtained with the BONELOAD script in MATLAB. (**D**) Muscle attachments of the skull used in the biomechanical simulations and the nodal restraint (red points) used for each biting scenario. C, canine; P, premolar; M, molar; i.t.m., internal pterygoid muscle (green); m.m., masseter muscle group (dark pink); t.m., temporalis muscle group (dark blue); t.m.j., temporo-mandibular joint; m.s., mandibular symphysis.

biting scenarios (Fig. 4B). This is agreeing with their high values in mΔSEa (Fig. 3A).

FEA without sinuses

The values of SE and ME obtained using FEA from 3D models of sinuses infilled computed for all biting scenarios at a gape angle of 12° (Fig. 2) are shown in tables S4 and S5. Removing the sinuses from 3D models allows us to quantify how large sinus cavities (i.e., empty spaces) and the resulting modification of skull geometry (i.e., the appearance of an external frontal dome) influence feeding biomechanics.

The difference between the values in ME obtained for the canine and second molar (mΔME), as well as the differences between the maximum and minimum values of adjusted SE across all teeth simulations (mΔSEa) for each species obtained from models without sinuses, is shown in table S7. The bivariate plot of mΔME on mΔSEa derived from FEA for all living bears without sinuses is shown in Fig. 3B. The values of mΔME for both living and extinct bears do not significantly change from the models with sinuses (Fig. 3 and tables S6 and S7). However, the values of mΔSEa among living bears range from 0.08 ± 0.01 for *U. americanus* to 0.48 ± 0.04 for *A. melanoleuca* (Fig. 3B). Notably, the mΔSEa values for cave bears without sinuses decrease to the level of living bears, which indicates that when sinuses are removed, the skull stiffness increases. The species that experiences the greatest decrease in mΔSEa values is *U. spelaeus ladinicus*, with a value of 0.25 ± 0.03, followed by *U. ingressus*, with a value of 0.30 ± 0.03. Therefore, as the values of mΔSEa are lower, this indicates few differences in SE when biting with different teeth.

The von Mises stress distribution across the skulls without sinuses in all living species shows that the stress is not homogeneously distributed, as it is mainly concentrated at the TMJ and at the posterior part of the rostrum (Fig. 5A). Among cave bears, as expected for their larger sinuses compared to living bears, the stress distribution is even more localized at the rostrum, which entails a low concentration of stress in the neurocranium and in the TMJ (Fig. 5B). Therefore, the level of von Mises stress obtained when biting from different teeth is more similar than in the models with sinuses (Fig. 4B).

Comparing FEAs with and without sinuses

Figure 6A shows the values of mΔSEa obtained by FEA in models with sinuses divided by the values of mΔSEa computed by FEA in

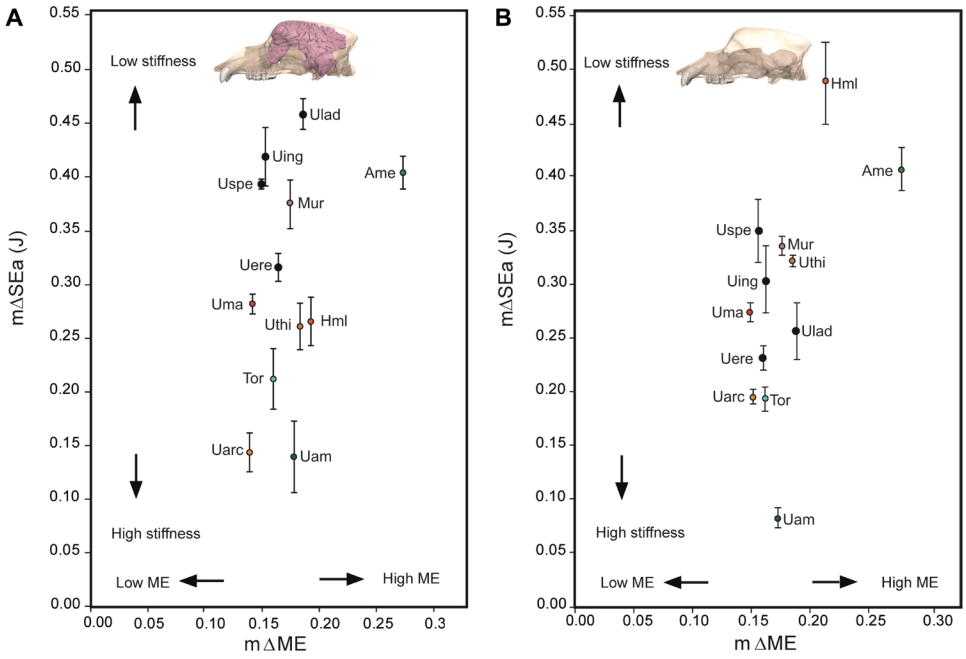

Fig. 3. Results of FEAs. (**A**) Bivariate plot of the maximum differences in ME (mΔME) and SE (mΔSEa) across the tooth loci simulations for each species obtained from models with sinuses. (**B**) Bivariate plot of the maximum differences in ME (mΔME) and SE (mΔSEa) across the tooth loci simulations for each species obtained from models without sinuses. Ame, *A. melanoleuca*; Hml, *H. malayanus*; Mur, *M. ursinus*; Tor, *T. ornatus*; Uam, *U. americanus*; Uarc, *U. arctos*; Uere, *U. eremus*; Uing, *U. ingressus*; Ulad, *U. spelaeus ladinicus*; Uspe, *U. spelaeus spelaeus*; Uthi, *U. thibetanus*.

models without sinuses (*i*mΔSEa) for the species sampled in a phylogenetic context. This index informs us on the gains/losses in mΔSEa (or skull stiffness) when sinuses are artificially removed (table S8). Comparing the values of *i*mΔSea, (i) *H. malayanus*, *U. arctos*, and *U. thibetanus* exhibit values of *i*mΔSEa < 1, suggesting that their sinuses increase their skull structural stability; (ii) *T. ornatus*, *U. americanus*, *M. ursinus*, and all the cave bears reach values of *i*mΔSEa > 1, suggesting that their sinuses decrease structural stability of their skull; (iii) *A. melanoleuca* and *Ursus maritimus* exhibit values of *i*mΔSEa ≈ 1, demonstrating a neutral effect of their sinuses in maintaining structural stability of their skulls while chewing.

The bivariate regression of the values of *i*mΔSEa against sinus volume relative to total skull volume (Fig. 5B and table S9) was significant ($r^2 = 0.6$, $P = 0.04$), indicating that the *i*mΔSEa is associated with sinus volume. In those species in which the sinuses increase structural stability (i.e., *i*mΔSEa < 1), their sinus volume does not exceed 25% of total skull volume (Fig. 6B). In contrast, in those species in which the sinuses decrease structural stability (i.e., *i*mΔSEa > 1), their sinus volume exceeds 25% of total skull volume (Fig. 6B).

A visual comparison of the results of the von Misses stress distribution across the skull in models with sinuses (Fig. 4) and without sinuses (Fig. 5) indicates that the distribution of the stress with sinuses is more homogeneous than in the models without sinuses in all species. This stress distribution difference is especially extreme in cave bears.

DISCUSSION

Sinus size and feeding biomechanics in living and extinct bears

The simulation of different chewing scenarios of skull models with sinuses (Figs. 3A and 4) and without sinuses (Figs. 3B and 5) using FEA allowed us to distinguish three groups of living bears depending on the effect of the sinuses on feeding biomechanics.

(i) Bears (*A. melanoleuca* and *U. maritimus*) in which the sinuses do not affect feeding biomechanics (those with *i*mΔSEa ≈ 1; Fig. 6, A and B). *U. maritimus* has relatively small sinuses (≈17% sinus volume/skull volume) without expanded frontal areas of the skull, which is also reflected in its moderately flattened forehead. This entails that the cranial geometry of *U. maritimus* is not compromised by sinus size. On the other hand, given that *U. maritimus* usually feeds primarily on blubber of prey much smaller than itself (*Phoca hispida* and *Erignathus barbatus*) (*17*), the actual biomechanical requirements of its skull are low. Therefore, the sinuses of *U. maritimus*, together with its vascular countercurrent system, are more involved in avoiding dehydration and freezing in the Arctic polar environment (*18*) than to provide structural stability and stress dissipation to the skull during feeding. Our results also support the hypothesis that the dietary specialization of *U. maritimus* decreases cranial functional performance (*19*).

The skull geometry of *A. melanoleuca* is optimized to confer structural stability (stiffness) by having a triangular section along the dorso-sagittal region of the skull as a consequence of a vertically directed temporalis muscle resembling the skull of the durophagous hyenas (*17*). This is also reflected in the similarity of sinus shape between *A. melanoleuca* and hyaenids (*20*). It is true that contrary to *A. melanoleuca*, the sinuses of hyaenids have an advantageous structure involved in dissipating the stresses generated during bone cracking (*21*), but while *A. melanoleuca* is adapted to feed with the post-carnassial dentition (*17*), hyaenids usually crack bones with the pre-carnassial dentition (i.e., premolars). Therefore, the specific skull geometry of *A. melanoleuca* confers enough integrity for the biomechanical demands required for feeding on bamboo. This explains the absence of changes in mΔSEa in the models with and without

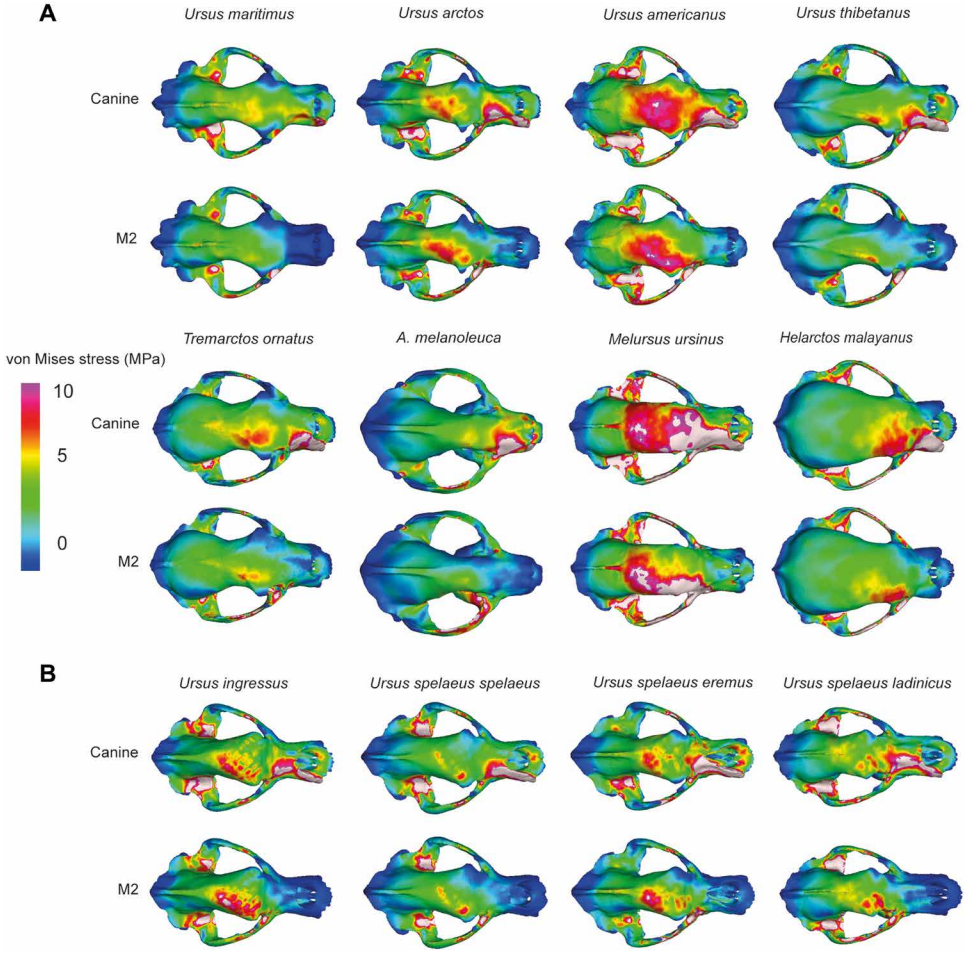

Fig. 4. Contour plots of von Mises stress distribution obtained from FEAs on each cranial model with sinuses. All models are obtained from each biting scenario for the right working side. (**A**) Cranial models of living bears. (**B**) Cranial models of cave bears. Only two chewing scenarios (canine and second upper molar) are shown for clarity.

sinuses (Figs. 3 and 6A). Moreover, the relatively small sinuses of *A. melanoleuca* (≈11% of sinus volume/skull volume; Fig. 6B) distribute homogenously the stresses between the rostrum and neurocranium (Figs. 4 and 5).

(ii) The sinuses of some bears (*H. malayanus*, *U. arctos*, and *U. thibetanus*) improve feeding biomechanics (those with *i*mΔSEa < 1), providing structural stability of the skull (high stiffness), as previously demonstrated for hyenas (*21*). This also applies to the large herbivorous marsupial *Diprotodon optatum*, as paranasal sinuses provide structural support, high bite forces, and low stresses while substantially lightening the skull (*22*). Moreover, their sinuses allow a more homogeneous distribution of stress across the skull. The models without sinuses concentrate the stress mainly on the rostrofrontal region and on the TMJ (Figs. 4A and 5A). Our results confirm the predictions made by Buckland-Wright (*23*) who proposed that the forces generated during biting must pass through the face anterior to the orbit and then run along the vaulted forehead to the sagittal crest (*21*). Accordingly, the sinuses play a key role for the load-bearing integration of the neurocranium and rostrum in this group of bears.

For *H. malayanus*, stress dissipation is necessary for opening hardwood trees in the search of insects such as beetle larvae or for breaking coconuts (*24*). Moreover, although the canines of sun bears seem to be adapted to accomplish these tasks (*24*), the external morphology of the skull does not appear to be equipped to perform these biomechanically demanding tasks. Both *U. arctos* and *U. thibetanus* are adapted to feed on high proportions of hard mast (<50% soft mast and >15% hard mast) compared to other bear species such as *U. americanus* or *T. ornatus* that usually feed on lower proportions of hard mast (feeding >50% soft mast and <15% hard mast), and therefore, they should require a skull less equipped to resist the forces generated during chewing (*24*). Mast refers to nuts, seeds, buds, and fruits of trees and shrubs.

Our results also show that these taxa have a relatively low sinus volume (i.e., less than 25% of sinus volume/skull volume; Fig. 6B), which leads to a moderately flattened forehead (see silhouettes in Fig. 6A), conferring structural stability when chewing and allowing effective stress dissipation. However, it should be noted that although *U. arctos* does not have sphenoidal sinuses developed in the frontal region or the TMJ, it has expanded sinuses along the dorso-sagittal section of the skull.

(iii) The sinuses in other living bears (*M. ursinus* and *U. americanus*) compromise feeding biomechanics (those with *i*mΔSEa > 1) by decreasing structural stability of the skull (high stiffness). This is also the case in *T. ornatus*, but its values of *i*mΔSEa are only slightly higher than one. This is notable because the main function of the sinuses is

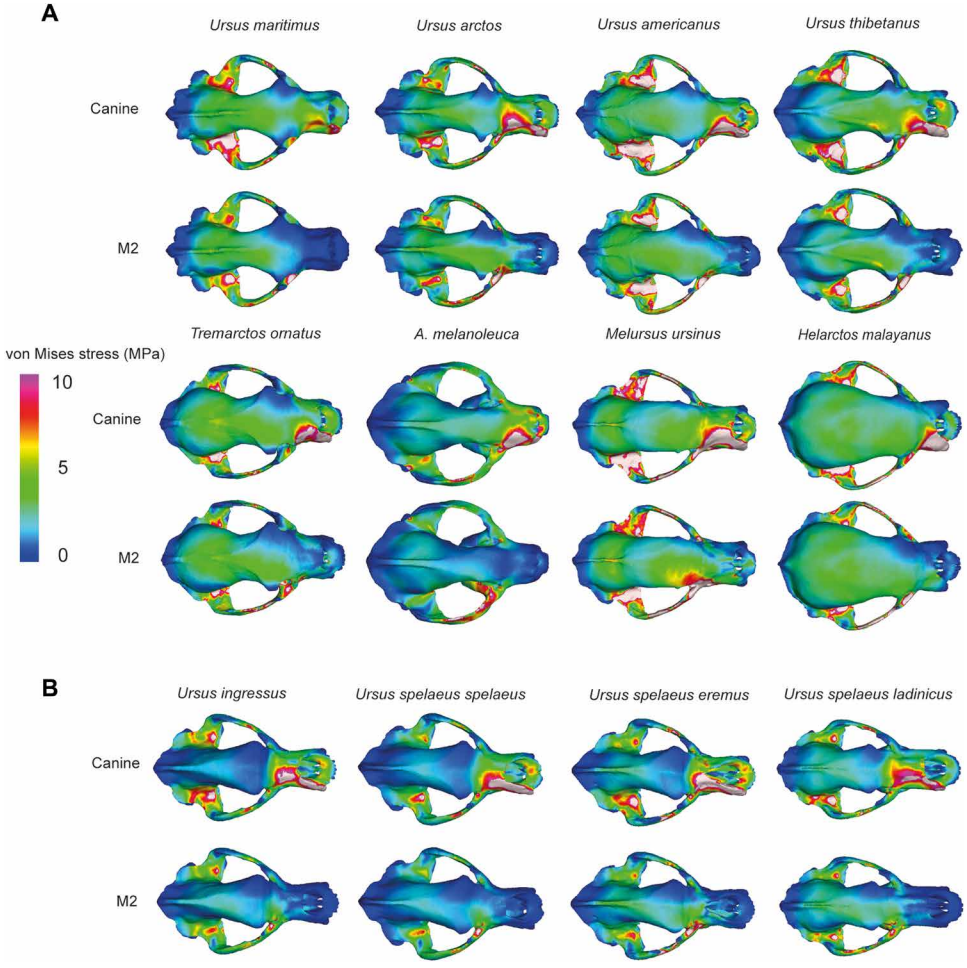

Fig. 5. Contour plots of von Mises stress distribution obtained from FEAs on each cranial model without sinuses. All models are obtained from FEAs of each chewing scenario for the right working side. (**A**) Cranial models of living bears. (**B**) Cranial models of cave bears. Only two chewing scenarios (canine and second upper molar) are shown for clarity.

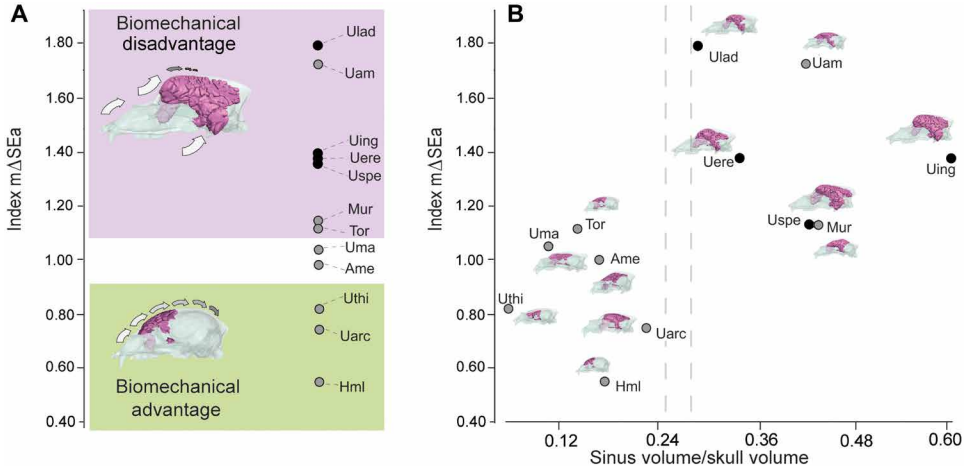

Fig. 6. Biomechanical effects of the paranasal sinuses. (**A**) Traitgram of the *im*ΔSEa (see text for details). Green branches represent those species in which the sinuses are advantageous, and those in blue represent those that the sinuses are disadvantageous. (**B**) Phylomorphospace of the bivariate plot depicted from the *im*ΔSEa against the relativized sinus volume to skull volume. In all cases, black circles represent extinct taxa, and gray circles represent living taxa. The virtual models of the sinuses analyzed are indicated in dark pink.

thought to be involved in stress dissipation during feeding and to provide skull structural stability (*20*–*22*). However, the analyses of von Mises stress in *M. ursinus* and *U. americanus* reveal higher stresses in models with sinuses than in models without sinuses (Figs. 4A and 5A), demonstrating that the sinuses have a minor role in the integration of the neurocranium and rostrum.

All cave bears, together with *U. americanus*, have the highest values of *i*mΔSEa index among the sample. This indicates that the sinuses compromise the feeding biomechanics of cave bears by decreasing structural stability of their skulls as observed in the biomechanical simulations outcomes of living *T. ornatus*, *M. ursinus*, and *U. americanus*. Moreover, the analyses of von Mises stress reveal that the sinuses produce much higher stresses during biting in all simulated scenarios than in living bears, including *U. americanus*, which results in a higher concentration of stress in the rostro-frontal region and in the TMJ (Figs. 4 and 5). This disadvantageous effect of the sinuses on feeding biomechanics is related with the acquisition of a highly relativized sinus volume (i.e., exceeding 25% of sinus volume/skull volume; Fig. 6B), which leads to a pronounced step in the forehead, often called the "frontal dome" that modifies the geometry of the skull (see silhouettes in Fig. 6). This is particularly extreme in cave bears, as they have greatly expanded sinuses (between 30% in *U. spelaeus ladinicus* and 60% in *U. ingressus* of sinus volume/skull volume; Fig. 6B). This frontal dome represents a diagnostic trait to distinguish brown bears from speleoid bears. However, the frontal dome impedes stress dissipation during chewing with the anterior dentition (Figs. 3, 4B, and 5B). Therefore, the sinuses in *T. ornatus*, *M. ursinus*, *U. americanus* and more particularly in cave bears lead to lower (and inefficient) stress dissipation between the rostrum and neurocranium as a consequence of the expansion in height of the frontal region of the skull. This also entails a decoupling between the rostrum and neurocranium on the role of stress dissipation. The relatively poor biomechanical capability for processing food using the anterior dentition would have affected hunting and foraging behavior that require forceful use of incisors and canines, for example, in hunting active prey, as in *U. arctos* (*24*).

Our results demonstrate that the highly developed sinuses in cave bears constrain their dietary flexibility as in the living *U. americanus*, which is the most herbivorous living bear inhabiting high latitudes (*25*). However, although *U. americanus* does not have a domed forehead to the same level as cave bears, its sinus volume is extremely large (Fig. 6B), which is enough to cause a disadvantageous effect on feeding biomechanics without having a modified skull geometry. Isotopic biochemistry studies [e.g., (*9*)] indicate that cave bears were fully herbivorous without the flexibility to shift their diet toward omnivory during the Pleistocene climatic cooling at the beginning of the Last Glacial Maximum (*10*). This was also supported by the analysis of tooth-root morphology in cave bears, as they tend to maximize tooth-root areas of their second upper molars toward an herbivorous diet (*24*). Therefore, if having large sinuses imposes a biomechanical restriction to feed on different resources in cave bears and *U. americanus*, why are large sinuses selected in these taxa?

Selective advantage of having large sinuses in bears: Hibernation length

Living bears such as the brown bear (*U. arctos*) and the American black bear (*U. americanus*) overcome winters in hibernation (*26*). In contrast, other bears do not hibernate (*U. maritimus*) or instead exhibit a facultative hibernation (*U. thibetanus*), i.e., a special type of lethargy (*27*). *U. thibetanus* only reduce their physical activity if the environmental conditions require it rather than to decrease their basal metabolism and body temperature (*28*). Neither *T. ornatus* nor *A. melanoleuca* hibernate, as both bears inhabit low-latitude ecosystems without severe winters.

Hibernation is the ability to stay in an energy-conserving state of torpor during the coldest months of the year when food is scarce or unavailable (*5*). During this time period, which can reach up to 6 months for some living bear species, the bear's metabolism changes to a special state by decreasing the basal metabolic rate [e.g., (*29*)]. As a consequence, a substantial decrease in heart rate is accompanied by a decrease in body temperature [e.g., (*30*)]. Accordingly, during this time, the bear does not drink, eat, urinate, or defecate: It survives by mobilizing its fat reserves acquired during the active period or predormancy (*26*).

The length of hibernation in living bears depends on several factors such as latitude and climate, rainfall, food availability, or sex (*26*). In cave bears, it is widely accepted that they had longer hibernation periods than living bears due to the length of the winters at those latitudes during the end of the Pleistocene (*3*–*5*, *11*). The physiology in animals that hibernate is mainly regulated by the activation of enzymes via stress pathways. Among these enzymes, the nitric oxide synthase (NOS) is activated when the concentration of CO_2 in blood increases (hypercapnia), and the levels of O_2 decrease (hypoxia) at the beginning of hibernation [e.g., (*31*)]. The response to these stimuli is to decrease body temperature, heart rate, and blood pressure (*32*). Recent studies link nitric oxide (NO) and hydrogen sulfide (HS) pathways with the control of the hibernation in bears, as these metabolites are related to the induction of several responses to stimuli of biological stress (*33*).

The production of NO and HS is segregated by the epithelium of the sphenoidal sinuses [e.g., (*12*–*14*)], and all the paranasal sinuses function as a reservoir for NO (*15*). With the exception of *M. ursinus*, the species that have large sinuses hibernate. *M. ursinus* and *U. americanus* have the lowest metabolic rates among living bears. While the low metabolic rate of *U. americanus* is related to hibernation, that of *M. ursinus* is mostly related to its low-energy diet based on insects (*34*). These observations are consistent with the key role of sinuses in lowering basal metabolic rates either to afford a low-energy diet (as in *M. ursinus*) or to hibernate (as in *U. americanus*). However, *U. arctos* hibernate, and it has a higher metabolic rate than *U. americanus*, but the predormancy period of *U. arctos* is comparatively longer than in *U. americanus* (*35*). The high metabolic rate of *U. arctos* compared to *U. americanus* also explains the fact that *U. arctos* is the only taxa among the sample that hibernates with sinus volume lower than 25% of skull volume. However, although neither sphenoidal sinuses across the TMJ or sinuses within the frontal dome are developed in brown bears, the frontal sinuses along the dorso-sagittal section are developed and may be involved in NO and HS sequestration but at a lower rate than in *U. americanus*. This disposition of the sinuses in *U. arctos* allows maintaining relatively long periods of hibernation without lacking the biomechanical flexibility to feed on different resources, including meat (*25*).

Sinuses, hibernation, and feeding biomechanics in cave bears

The 3D biomechanical simulations of different chewing scenarios demonstrate that cave bears lack the degree of biting efficiently with all teeth, leading to an absence of the dietary flexibility of the omnivorous *U. arctos*—i.e., their closest living relative. Moreover, this lack of dietary flexibility is associated with having expanded sinuses

in the frontal region, which forms the domed forehead that characterizes the speloid lineage. This dome greatly reduces the dissipation of stress when biting with the anterior dentition and hence forced cave bears to have a skull biomechanically constrained for chewing vegetal matter with their posterior teeth, as in the living *U. americanus* (*24*). However, it could also be argued that the evolution of the domed skull and enlarged sinuses in cave bears was secondary (or simultaneous) to the evolution of their restricted herbivorous diet and possibly a necessity following their low energetic diets and inability to forage during cold temperatures with low vegetation productivity. On the other hand, the selective advantage of having extremely large sinuses in cave bears is probably related to their necessity to overcome long winters in hibernation of the Last Glacial, with the hibernation process largely controlled by various enzymes segregated in the sphenoidal sinuses (*12*–*15*). We hypothesize that this was the key selective agent to increase sinus size along the evolutionary history of the speloid lineage. At the same time, the large sinuses of cave bears caused a life history trade-off between feeding and hibernation.

Our study demonstrates that the anatomical specialization in cave bears for longer hibernation periods is associated with the lack of dietary flexibility in cave bears by having a restricted low energetic, herbivorous diet constrained biomechanically by skulls less able to dissipate biting stress. If this lack of dietary flexibility precluded cave bears to acquire sufficient fat storage to overcome the extreme winters of the Late Pleistocene, cooling in hibernation remains a tantalizing question. However, the new findings of this study demonstrate that both the necessity of having long periods of hibernation and their restricted herbivorous diet are likely to be a more critical factor in the decline and ultimate extinction of the cave bear than previously suspected. Our new life history trade-off hypothesis also formulates a specific, mechanistic pathway by which climatic changes during the Last Glacial could have directly influenced the ability of some members of the Ice Age megafauna to obtain adequate nutrients and successfully survive during the extreme ecological conditions of the coldest months.

MATERIALS AND METHODS

Twelve skulls of living and extinct bears were computed tomography (CT)–scanned from different museums (table S1). Of them, eight skulls belong to living bears (*U. arctos*, *U. maritimus*, *U. americanus*, *U. thibetanus*, *M. ursinus*, *H. malayanus*, *T. ornatus*, and *A. melanoleuca*), and four skulls belong to extinct Pleistocene species/subspecies of the cave bear complex (*U. spelaeus* sensu lato): *U. spelaeus spelaeus*, *U. spelaeus ladinicus*, *U. spelaeus eremus*, and *U. ingressus* (Fig. 1 and table S1).

FEA of the skull with sinuses

The CT stacks were processed (see the Supplementary Materials) to obtain meshes of the 3D models that were imported into Strand7 Release 2.4.6 (Strand7 Pty Ltd., Sydney, Australia). We removed the duplicated nodes of the meshes and produced coarse-, medium-, and fine-resolution solid meshes following (*16*). The centroids of each muscular insertion and the subsequent force vectors, essential for the biomechanical calculations, were calculated using BONELOAD (*36*) from 3D mandibular models (Fig. 2).

We calculated the insertion surface areas in the skull of masticatory muscles (temporalis, masseter, and medial pterygoid groups; Fig. 2) using Strand7 Release 2.4.6. These surface areas (Fig. 2) were delimited using bony rugosities and comparative anatomical studies. To calculate the input muscle force, we followed the dry skull method (*37*). The muscle forces were adjusted to reflect differential activation between the working (biting) and balancing side, with the balancing side muscle forces adjusted to 60% of maximum forces estimated for the working side.

Last, the centroids of the attachment areas of masticatory muscles on the mandible and the muscle attachment sites for both the mandible and the cranium for the left and right temporalis, masseter, and medial pterygoid group (Fig. 2) were imported into the BONELOAD script in MATLAB software to distribute the calculated muscle forces over the attachment areas using the tangential forces (*36*).

We used three nodal constrains on the 3D models: left and right TMJs (center of the condylar process) plus the unilateral bite point, the latter depending on each simulated scenario: left and right upper canines (C), fourth upper premolar (P4), first upper molar (M1), and second upper molar (M2) (Fig. 2). The unilateral bite points were placed at the center of the occlusal surface of the tooth, except for P4, where a single nodal constraint was placed on the top of the tallest cusp (Fig. 2). Accordingly, while the nodal constraint of the TMJ on the working side prevents translational movement in all three axes, the constraint of the TMJ on the balancing side allows translation along the axis of the joint. All the biting scenario models were simulated at a chewing scenario of 12° of gape angle. Moreover, in all the models, we used isotropic material properties with Young's modulus of 18 GPa and a Poisson's ratio of 0.3 (*38*).

We measured nodal reaction forces at the nodal constraint of each tooth in the respective biting scenarios, and the values of SE (is a measure of stiffness or structural stability) were calculated from all simulations. We also obtained the ME [i.e., the nodal reaction force divided by the total input muscle force (average of all the forces of each muscle on both the right and left sides)]. Following this, we averaged the values of ME and SE of both left and right sides in coarse-, medium-, and high-resolution models for each skull. The total SE values for each biting simulation were adjusted to the cranial volume (VA) and total input force (FA) according to the equation of (*38*). We used the brown bear (*U. arctos*) as the adjusted reference because it is the closest living relative of the cave bear and has a generalist omnivorous diet.

FEA of the skull without sinuses

To test whether the extremely developed sinuses in the cave bear influence its biomechanical performance for feeding behavior, we eliminated virtually the paranasal sinuses by filling the cavities with artificial bone material using Geomagic (*21*, *22*). The sinuses have a potential dual effect on feeding biomechanics (i) for having large empty spaces in the paranasal cavities and (ii) for the appearance of a dome as a consequence of sinus inflation on the frontal area. Therefore, removing the sinuses from 3D models allows us to quantify the effects of (i) having large empty spaces plus skull geometry together (the appearance of a frontal dome) and (ii) the frontal dome on skull geometry.

We considered as paranasal sinuses the ethmoid, frontal, and sphenoid sinuses. We excluded the maxillary sinuses because they are not included within the frontal dome. This terminology is related to the bone from which the cavity is generated. We calculated in each specimen the volume of the sinuses to quantify the degree of the development of the paranasal sinuses in cave bears relative to living bears.

Each model without sinuses was imported into Strand7, and we computed the same process for FEA as for the original models with paranasal structures (i.e., not filled cavities). We also calculated the ME and SE for each model without sinuses, and we compared the effects of having sinuses on feeding biomechanics for each bear species, including living and extinct forms. In total, our analyses comprised a total of 576 simulations, one per each tooth (C, P4, M1, and M2) on both sides (left and right) and on models with and without sinuses.

Comparing the effects of paranasal sinuses in feeding biomechanics

To compare the effect of the paranasal sinus on skull biomechanics, we divided the mΔSEa values obtained in the biomechanical simulations with sinuses for all feeding scenarios to the mΔSEa values obtained in the simulations without sinuses (hereafter named as index mΔSEa). Accordingly, when this ratio is >1, it means that the biomechanical simulations with sinuses have higher values of mΔSEa than in the biomechanical simulations without sinuses, which indicates that the sinuses have a disadvantageous effect given that the structural integrity of the skull (or stiffness) is lower when having sinuses. In contrast, when this ratio is <1, it means that the biomechanical simulations with sinuses have lower values of mΔSEa than in the simulations without sinuses. This suggests that the sinuses have an advantageous effect on feeding biomechanics given that the structural integrity of the skull (or stiffness) is higher when having sinuses. Last, when this ratio is close to 1, it indicates that the sinuses have a neutral effect on feeding biomechanics.

We regressed the volume of the sinuses adjusted to the total cranial volume against the difference of SE obtained in both sets of analyses (i.e., difference between the SE values obtained from the FEAs computed on the models with and without sinuses for each skull). We used ordinary least squares regression analysis computed with the software PAST version 3.15 (*39*).

SUPPLEMENTARY MATERIALS

Supplementary material for this article is available at http://advances.sciencemag.org/cgi/content/full/6/14/eaay9462/DC1

View/request a protocol for this paper from *Bio-protocol*.

REFERENCES AND NOTES

1. B. Kurtén, *The Cave Bear Story: Life and Death of a Vanished Animal* (Columbia Univ. Press, 1976), p. 163.
2. G. G. Fortes, A. Grandal-d'Anglade, B. Kolbe, D. Fernandes, I. N. Meleg, A. García-Vázquez, A. C. Pinto-Llona, S. Constantin, T. J. de Torres, J. E. Ortiz, C. Frischauf, G. Rabeder, M. Hofreiter, A. Barlow, Ancient DNA reveals differences in behaviour and sociality between brown bears and extinct cave bears. *Mol. Ecol.* **25**, 4907–4918 (2016).
3. M. Pérez-Rama, D. Fernández-Mosquera, A. Grandal-d'Anglade, Effects of hibernation on the stable isotope signatures of adult and neonate cave bears. *Quaternaire* **4**, 79–88 (2011).
4. M. Pacher, A. J. Stuart, Extinction chronology and palaeobiology of the cave bear *(Ursus spelaeus)*. *Boreas* **38**, 189–206 (2009).
5. A. Grandal-d'Anglade, M. Pérez-Rama, A. García-Vázquez, G. M. González-Fortes, The cave bear's hibernation: Reconstructing the physiology and behaviour of an extinct animal. *Hist. Biol.* **31**, 429–441 (2019).
6. S. C. Münzel, M. Stiller, M. Hofreiter, A. Mittnik, N. J. Conard, H. Bocherens, Pleistocene bears in the Swabian Jura (Germany): Genetic replacement, ecological displacement, extinctions and survival. *Quatern. Int.* **245**, 225–237 (2011).
7. S. C. Münzel, N. J. Conard, Cave bear hunting in the Hohle Fels, a cave site in the Ach Valley, Swabian Jura. *Rev. Paléobiol.* **23**, 877–885 (2004).
8. M. Baca, D. Popović, K. Stefaniak, A. Marciszak, M. Urbanowski, A. Nadachowski, P. Mackiewicz, Retreat and extinction of the Late Pleistocene cave bear (Ursus spelaeus sensu lato). *Sci. Nat.* **103**, 92 (2016).
9. H. Bocherens, Isotopic insights on cave bear palaeodiet. *Hist. Biol.* **31**, 410–421 (2019).
10. G. Terlato, H. Bocherens, M. Romandini, N. Nannini, K. A. Hobson, M. Peresani, Chronological and Isotopic data support a revision for the timing of cave bear extinction in Mediterranean Europe. *Hist. Biol.* **31**, 474–484 (2019).
11. M. Stiller, G. Baryshnikov, H. Bocherens, A. G. d'Anglade, B. Hilpert, S. C. Münzel, R. Pinhasi, G. Rabeder, W. Rosendahl, E. Trinkaus, M. Hofreiter, M. Knapp, Withering away—25,000 years of genetic decline preceded cave bear extinction. *Mol. Biol. Evol.* **27**, 975–978 (2010).
12. J. O. Lundberg, Nitric oxide and the paranasal sinuses. *Anat. Rec.* **291**, 1479–1484 (2008).
13. K. Petruson, J. Stalfors, K. E. Jacobsson, L. Ny, B. Petruson, Nitric oxide production in the sphenoidal sinus by the inducible and constitutive isozymes of nitric oxide synthase. *Rhinology* **43**, 18–23 (2005).
14. C. H. Yan, S. Hahn, D. McMahon, D. Bonislawski, D. W. Kennedy, N. D. Adappa, J. N. Palmer, P. Jiang, R. J. Lee, N. A. Cohen, Nitric oxide production is stimulated by bitter taste receptors ubiquitously expressed in the sinonasal cavity. *Am. J. Rhinol. Allergy* **31**, 85–92 (2017).
15. J. A. Andersson, A. Cervin, S. Lindberg, R. Uddman, L. O. Cardell, The paranasal sinuses as reservoirs for nitric oxide. *Acta Otolaryngol.* **122**, 861–865 (2002).
16. Z. J. Tseng, J. J. Flynn, Structure-function covariation with nonfeeding ecological variables influences evolution of feeding specialization in Carnivora. *Sci. Adv.* **4**, eaao5441 (2018).
17. B. Figueirido, Z. J. Tseng, A. Martín-Serra, Skull shape evolution in durophagous carnivorans. *Evolution* **67**, 1975–1993 (2013).
18. A. S. Blix, Adaptations to polar life in mammals and birds. *J. Exp. Biol.* **219**, 1093–1105 (2016).
19. G. J. Slater, B. Figueirido, L. Louis, P. Yang, B. Van Valkenburgh, Biomechanical consequences of rapid evolution in the polar bear lineage. *PLOS ONE* **5**, e13870 (2010).
20. A. A. Curtis, B. Van Valkenburgh, Beyond the sniffer: Frontal sinuses in Carnivora. *Anat. Rec. (Hoboken)* **297**, 2047–2064 (2014).
21. J. B. Tanner, E. R. Dumont, S. T. Sakai, B. L. Lundrigan, K. E. Holekamp, Of arcs and vaults: The biomechanics of bone-cracking in spotted hyenas (*Crocuta crocuta*). *Biol. J. Linn. Soc.* **95**, 246–255 (2008).
22. A. C. Sharp, T. H. Rich, Cranial biomechanics, bite force and function of the endocranial sinuses in Diprotodon optatum, the largest known marsupial. *J. Anat.* **228**, 984–995 (2016).
23. J. C. Buckland-Wright, Bone structure and the patterns of force transmission in the cat skull (*Felis catus*). *J. Morphol.* **155**, 35–61 (1978).
24. A. Pérez-Ramos, K. Kupczik, A. H. Van Heteren, G. Rabeder, A. Grandal-D'Anglade, F. J. Pastor, F. J. Serrano, B. Figueirido, A three-dimensional analysis of tooth-root morphology in living bears and implications for feeding behaviour in the extinct cave bear. *Hist. Biol.* **31**, 461–473 (2019).
25. K. Bojarska, N. Selva, Spatial patterns in brown bear *Ursus arctos* diet: The role of geographical and environmental factors. *Mammal Rev.* **42**, 120–143 (2012).
26. E. C. Hellgren, Physiology of hibernation in bears. *Ursus* **10**, 467–477 (1998).
27. S. Sathyakumar, L. K. Sharma, S. A. Charoo. Ecology of Asiatic black bear (*Ursus thibetanus*) in Dachigam National Park, Kashmir, India (Final Project Report, Wildlife Institute of India, 2013) p. 169.
28. P. D. Watts, N. A. Øritsland, R. J. Hurst, Standard metabolic rate of polar bears under simulated denning conditions. *Physiol. Zool.* **60**, 687–691 (1987).
29. R. A. Nelson, H. W. Wahner, J. D. Jones, R. D. Ellefson, P. E. Zollman, Metabolism of bears before, during, and after winter sleep. *Am. J. Physiol.* **224**, 491–496 (1973).
30. Ø. Tøien, J. Blake, D. M. Edgar, D. A. Grahn, H. C. Heller, B. M. Barnes, Hibernation in black bears: Independence of metabolic suppression from body temperature. *Science* **331**, 906–909 (2011).
31. D. J. O'Hearn, G. D. Giraud, J. M. Sippel, C. Edwards, B. Chan, W. E. Holden, Exhaled nasal nitric oxide output is reduced in humans at night during the sleep period. *Resp. Physiol. Neurobi.* **156**, 94–101 (2007).
32. R. K. Kudej, C. Depre, NO with no NOS in ischemic heart. *Cardiovasc. Res.* **74**, 1–3 (2007).
33. I. G. Revsbech, X. Shen, R. Chakravarti, F. B. Jensen, B. Thiel, A. L. Evans, J. Kindberg, O. Fröbert, D. J. Stuehr, C. G. Kevil, A. Fago, Hydrogen sulfide and nitric oxide metabolites in the blood of free-ranging brown bears and their potential roles in hibernation. *Free Radic. Biol. Med.* **73**, 349–357 (2014).
34. B. K. McNab, Rate of metabolism in the termite-eating sloth bear (*Ursus ursinus*). *J. Mammal.* **73**, 168–172 (1992).
35. G. Brown, *The Great Bear Almanac* (Lyons and Burford, 1993), p. 325.
36. I. R. Grosse, E. R. Dumont, C. Coletta, A. Tolleson, Techniques for modeling muscle-induced forces in finite element models of skeletal structures. *Anat. Rec. (Hoboken)* **290**, 1069–1088 (2007).
37. J. J. Thomason, Cranial strength in relation to estimated biting forces in some mammals. *Can. J. Zool.* **69**, 2326–2333 (1991).
38. E. R. Dumont, J. Piccirillo, I. R. Grosse, Finite element analysis of biting behaviour and bone stress in the facial skeletons of bats. *Anat. Rec. Part A Discov. Mol. Cell Evol. Biol.* **283**, 319–330 (2005).

39. Ø. Hammer, D. A. Harper, P. D. Ryan, PAST: Paleontological statistics software package for education and data analysis. *Palaeontol. Electron.* **4**, 9 (2001).
40. K. K. Yee, B. A. Craven, C. J. Wysocki, B. Van Valkenburgh, Comparative morphology and histology of the nasal fossa in four mammals: Gray squirrel, bobcat, coyote, and white-tailed deer. *Anat. Rec. (Hoboken)* **299**, 840–852 (2016).

Acknowledgments: We are especially grateful to C. M. Janis for her insightful comments on an earlier version of this manuscript. Two anonymous reviewers and the associate editor (D. Erwin) contributed insightful suggestions to improve the manuscript. **Funding:** This study was supported by the Spanish Ministry of Economy and Competitiveness (MINECO) (grants CGL2012-37866 and CGL2015-68300P to B.F.). A.P.-R. is an FPI fellow of the Spanish MINECO (BES-2013-065469) associated to the project (CGL2012-37866) of B.F. A.G.D. was granted by a Spanish MINECO project (CGL2014-57209-P). **Author contributions:** A.P.-R. and B.F. designed research. A.P.-R., F.J.P., G.R., A.G.-D., and B.F. collected data. Z.J.T. and A.P.-R. performed FEAs. Z.J.T. and A.G.-D. assisted with writing. A.P.-R. and B.F. wrote the paper. **Competing interests:** The authors declare that they have no competing interests. **Data and materials availability:** All data needed to evaluate the conclusions in the paper are present in the paper and/or the Supplementary Materials. Additional data related to this paper may be requested from the authors.

Submitted 6 August 2019
Accepted 9 January 2020
Published 1 April 2020
10.1126/sciadv.aay9462

Citation: A. Pérez-Ramos, Z. J. Tseng, A. Grandal-D'Anglade, G. Rabeder, F. J. Pastor, B. Figueirido, Biomechanical simulations reveal a trade-off between adaptation to glacial climate and dietary niche versatility in European cave bears. *Sci. Adv.* **6**, eaay9462 (2020).